Optical Ray Tracer Summary Report

Yuet Long Lai
Blackett Laboratory, Imperial College London, SW7 2AZ, UK

***Abstract*—We report that the ray tracer is functioning properly, and that it successfully converges light rays and focus on the focal plane. Moreover, we report that the ray tracer demonstrated the plano-convex lens has a less spherical aberration effect when the convex side is facing the input, and that the optimised lens has curvatures of $1.129 \cdot 10^{-2} mm^{-1}$ and $-8.283 \cdot 10^{-3} mm^{-1}$ for the first and second surface respectively.**

I. Introduction

THIS report investigates the optical ray tracer constructed according to the the project script. We will discuss the specific techniques used to execute the code that is not mentioned in the project script, the findings and the expected results as well as the performance of our lens made through the code.

II. Method

Due to the fact that our surface for refraction can have curvature of either positive, negative or zero (flat surface), I designed the code with 3 if-else statement such that it accounts for all 3 cases in both the intercept and propagate ray methods in my class for spherical refraction. For the cases of positive and negative curvature, l was found as instructed in the Task 4 and select the correct l value. However, for the flat surface case, an equation is derived by resolving vectors to find the value of l in this case:

$$P_z + l\hat{k_z} = z_0 \tag{1}$$

where P_z is the z-component of the point of the ray and $\hat{k_z}$ is the z-component of the unit vector of direction, and z_0 is the position of the lens on the z-axis.

For the refraction method according to Task 5, the vector form of Snell's Law [1] was used to directly find the new direction of the ray after the refraction. The equation is as follow:

$$\mathbf{k_2} = \frac{n_1}{n_2}\mathbf{k_1} + \mathbf{n}\left(-\frac{n_1}{n_2}\mathbf{n}\cdot\mathbf{k_1} - \sqrt{1-(\frac{n_1}{n_2})^2(1-(\mathbf{n}\cdot\mathbf{k_1})^2)}\right) \tag{2}$$

where $\mathbf{k_1}$ and $\mathbf{k_2}$ are the initial and final direction vectors of the ray, n_1 and n_2 are the refractive indices and $\mathbf{n}$ is the normal vector of the refracting surface at the point of intercept. $\mathbf{k_2}$ was normalised after using this Eq.2.

In order to facilitate initialisation of a beam of light shining towards a proper lens with more than one surface, a new class is created and a few methods are created for adding how many refractive surface you want (supposedly 2 surfaces) and an output plane, to propagate the rays and plot the ray traces and the spot diagrams, and to find the RMS spot radius and estimate the focus of the lens. Moreover, a beam of ray of uniform density was generated by making the arc length between two ray point constant. In my code, I defined that arc length to be the arc length between $\frac{\pi}{3}$ radians at diameter of $1mm$. Since $l = \frac{d}{2}\theta$, $\theta_d = \frac{2\pi}{(\pi d)/(\pi/6)} = \frac{\pi}{3d}$ where d is the diameter of the beam. Therefore, the number of sectors needed as a function of diameter would be $N_{sector} = 6d$ (N_{sector} is the number of sectors). This relation was then used to generate a beam of rays of uniform density using 2 for loops.

III. Testing

After establishing the code necessary for the lens system to run, A few test rays are propagated to see if it works. And as you can see in Fig. 1, the rays are refracting the way it is expected to.

The position of the paraxial focus was found by using the ray $0.1mm$ above optical axis, and the estimation of it was done through a straight line equation between the intercept on the lens and intercept on output plane. The expected value of the paraxial focal length is given as follow [2]:

$$f = \frac{n_2 R}{n_2 - n_1} \tag{3}$$

where f is the expected paraxial focal length, n_1 and n_2 the refractive indices and R the radius of the spherical surface, which is the reciprocal of the curvature. Both the estimation and the expected values of paraxial focal length are $100.0mm$, which shows that the expected value agrees with the measure value of focal length (Technically the estimated value is $99.9998mm$, which means there is a $2 \cdot 10^{-4}\%$ error, but since it is a very small error, it would be unreasonable to include this many significant figures).

After confirming the value of focal length for the single spherical surface, two pairs of parallel rays in different directions were plotted to see if they focus on the same output plane, which in this case would sit at $z = 200mm$. In Fig. 2a, the two pairs of rays in colour red and blue both converge at the output plane at $z = 200m$ as expected, and in Fig. 2b, 3 pairs of parallel rays with various distance from the optical axis were propagated through the refracting surface and it is evident that it was showing effects of spherical aberration due to the difference in where on the z-axis do the pairs of rays focus at.

IV. Investigation

A. Single Spherical Surface

A beam of rays horizontal to the optical axis was propagated towards the same single spherical surface in the above parts in Fig. 3a. As you can see, the light rays are behaving as expected: the rays converge at $z = 200mm$, where the focal

point was estimated and expected to be at. However, spherical aberration is also expected from this system. Using the plot on the right in Fig. 3b, the RMS spot radius and the size of geometrical focus are calculated to be $2.004 \cdot 10^{-3}mm$ and $1.261 \cdot 10^{-5}mm^2$. Using the definition of diffraction limit from the project script, using $\lambda = 558nm$ for the calculation, the diffraction limit gives a value of $11.16 \cdot 10^{-3}mm$. The RMS spot radius or even spot diameter is smaller than the diffraction limit, therefore meaning that if we take effects of diffraction into account, the spherical aberration is not severe enough to dominate or overcome the effects of diffraction, i.e. whether or not the size of the geometrical focus is bigger than the size of the Airy disk [3].

It is the same case in Fig. 4, except that there is a downward displacement by $4mm$ for the beam and they initialise with a direction of 0.05 in the x-direction also. In4b, the spot diagram is showing a significant amount coma, which is expected if the incoming ray travels into the lens at an angle [4].

B. Plano-Convex Lens

As we can see in Fig. 5, the plano-convex lens in both orientation focus the beam of light pretty well, with a certain amount of spherical aberrations of course. They also have a slight difference in the focal length. The results are presented in Table I:

Plano-Convex Lens	RMS spot radius (mm)	Geometrical Focus Size (mm^2)	Focal length (mm)
Convex side facing input	$8.359 \cdot 10^{-3}$	$2.195 \cdot 10^{-4}$	95.95
Plane side facing input	$3.330 \cdot 10^{-2}$	$3.484 \cdot 10^{-3}$	99.25

TABLE I: Spherical Aberration results for plano-convex lens in both orientation

As we can see, the plano-convex lens with convex side facing input has a lower RMS spot radius value and geometrical focus size, meaning that it has less spherical aberration impacting the system. This is because the parallel rays hat are near the edge of the lens diffract through a much smaller angle, and therefore giving a less deviation in the focal point, hence a smaller RMS radius and a smaller spherical aberration effect [5].

We can also see the difference between the effect of the orientation of the same lens by comparing the RMS spot radius values to diffraction limits of the corresponding diameter of the beam. In Fig. 6, firstly you can see that the RMS spot radius values shoots up much more when the plane side is facing the input as diameter of the beam increase, meaning that this orientation of the plano-convex lens is more susceptible to the effect of spherical aberration. In addition, you can see that the points for the lens' plane side facing the input exceeds the diffraction limits much quicker.

Also, using the lensmaker formula $\frac{1}{f} = (n-1)(\frac{1}{R_1} - \frac{1}{R_2} + \frac{(n-1)d}{nR_1R_2})$, the expected focal length for both the orientation of the lens is $96.75mm$, which means for the plano-convex lens with convex side facing input, its measured focal length (measured by finding the z-axis intercet between the point of intercept on the output plane and the point of intercept on the second surface of the lens) has a 0.8261% error, and for the lens with plane side facing input a 2.585% error.

C. Optimisation

Using the optimize.fmin_tnc function from scipy, with initial guesses for the curvatures be $1.0 \cdot 10^{-3}mm^{-1}$ and $-1.0 \cdot 10^{-3}mm^{-1}$ and setting the focal plane to be at focal length of $100mm$, the optimised values for the curvatures of the first and second surface of the lens are $1.129 \cdot 10^{-2}mm^{-1}$ and $-8.283 \cdot 10^{-3}mm^{-1}$ respectively, with a RMS spot radius of $3.264 \cdot 10^{-3}mm$. However, note that the initial guess for the curvatures affects the optimised values. Therefore, another approached is used. Using the same function, a contour plot (see Fig. 7) is plotted to investigate the relationship between the combinations of curvatures and the corresponding RMS spot radius values. As you can see in Fig. 7b, there is a deep purple region in which a RMS spot radius value of below $1.05 \cdot 10^{-3}mm$ can be achieved, resulting in a small effect of spherical aberration and therefore can optimise the lens' performance. Furthermore, in Fig. 7b, a more in depth demonstration of the contours within the valley is shown, you can see there are a number of small minimas lying within the valley. Those values can be extracted and be used to optimise the lens further.

If timing allows, instead of doing a contour plot, a 3D plot can be attempted in order to have a better view, and potentially find a set of values of curvatures that all optimise the lens.

V. Conclusion

In conclusion, the optical ray tracer performed within the expectation. It demonstrated accurately how a rays would travel in a lens system, and that the effect of spherical aberrations due to orientation of the plano-convex lens, and that the measured values for focal lengths match the predictions. Moreover, we optimised the lens with a curvature combination of $1.129 \cdot 10^{-2}mm^{-1}$ and $-8.283 \cdot 10^{-3}mm^{-1}$ with a RMS spot radius of $3.264 \cdot 10^{-3}mm$, and we discovered that there can be multiple of combinations of curvatures of the lens that can give us a better optimised lens using contour maps.

References

[1] B. de Greve, 'Reflections and Refractions in Ray Tracing', 13 Nov. 2006. Available: https://graphics.stanford.edu/courses/cs148-10-summer/docs/2006–degreve–reflection_refraction.pdf. (accessed: 8 Dec. 2021)

[2] K. Gibbs, 'Focal length and magnification of a spherical surface', 2011. Available: https://www.schoolphysics.co.uk/age16-19/Optics/Refraction/text/Spherical_surfaces/index.html (accessed Dec. 08, 2021).

[3] Edmund Optics, 'The Airy Disk and Diffraction Limit'. Available: https://www.edmundoptics.co.uk/knowledge-center/application-notes/imaging/limitations-on-resolution-and-contrast-the-airy-disk/ (accessed Dec. 08, 2021).

[4] Hyperphysics, 'Coma and Astigmatism'. Available: http://hyperphysics.phy-astr.gsu.edu/hbase/geoopt/coma.html (accessed Dec. 08, 2021).

[5] Kullabs, 'Spherical Aberration in a Lens and Scattering of Light'. Available: https://kullabs.com/class-11/physics-11/dispersion-of-light/spherical-aberration-in-a-lens-and-scattering-of-light (accessed Dec. 08, 2021).

VI. Figures

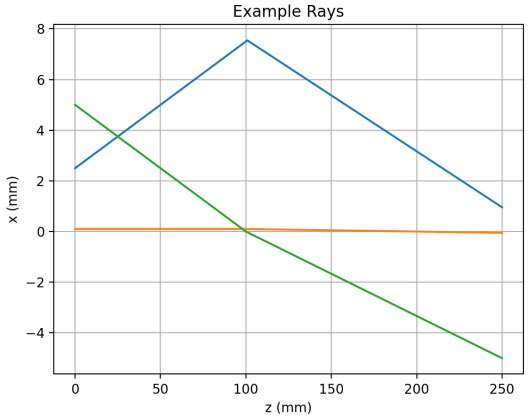

Fig. 1: Tracing a few example rays through the single spherical surface to test if the system works

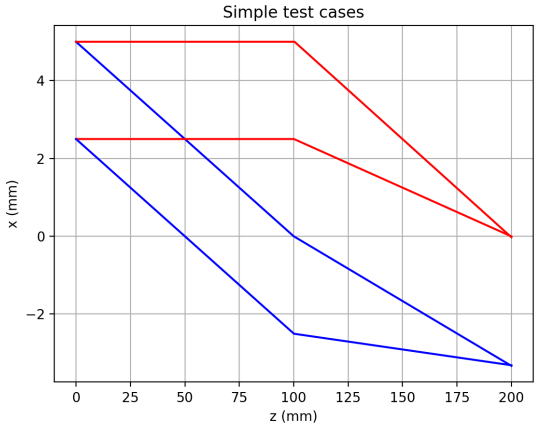

(a) Test case that shows parallel rays in different directions both focus on the same focal plane.

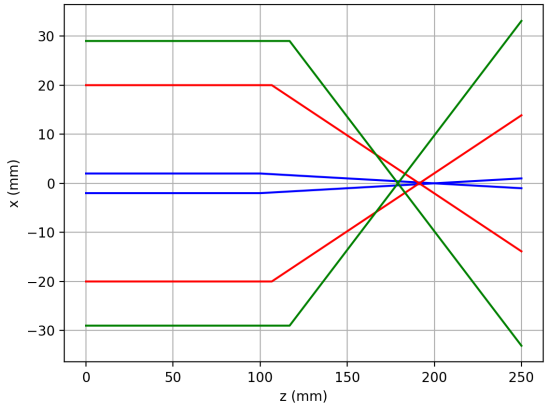

(b) Test case that shows immense effect of spherical aberration.

Fig. 2: Other simple testing cases for the refracting surface

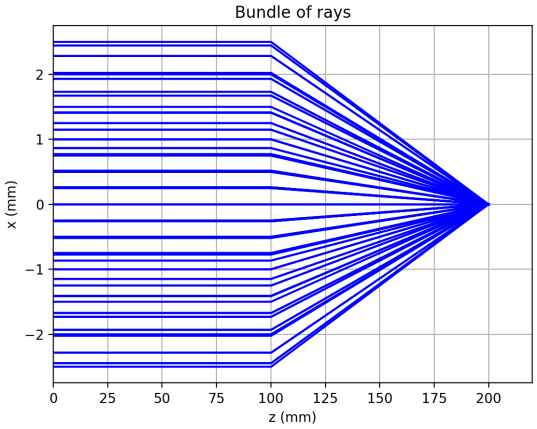

(a) Propagating a beam of rays towards the single spherical surface

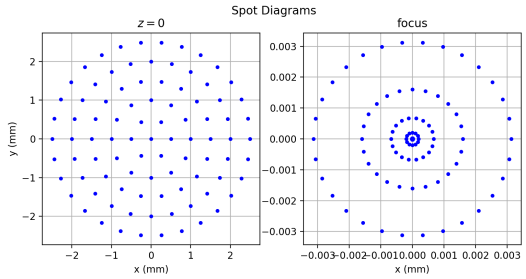

(b) Spot Diagram for the beam in Fig. 3a

Fig. 3: A Ray diagram of a beam of light going through a single spherical surface and the corresponding spot diagrams

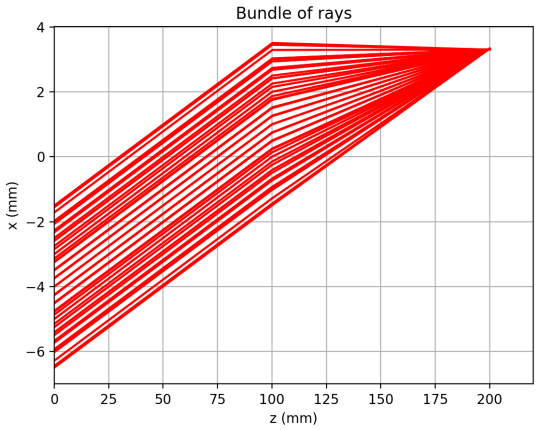

(a) Propagating a beam of rays towards the single spherical surface at an angle and a downwards displacement

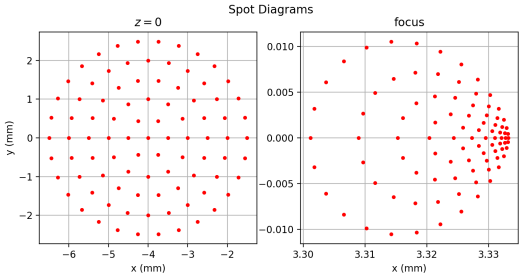

(b) Spot Diagram for the beam in Fig. 4a. Note that the spot diagram at the focal plane is a coma.

Fig. 4: A Ray diagram of a beam of light going through a single spherical surface and the corresponding spot diagrams

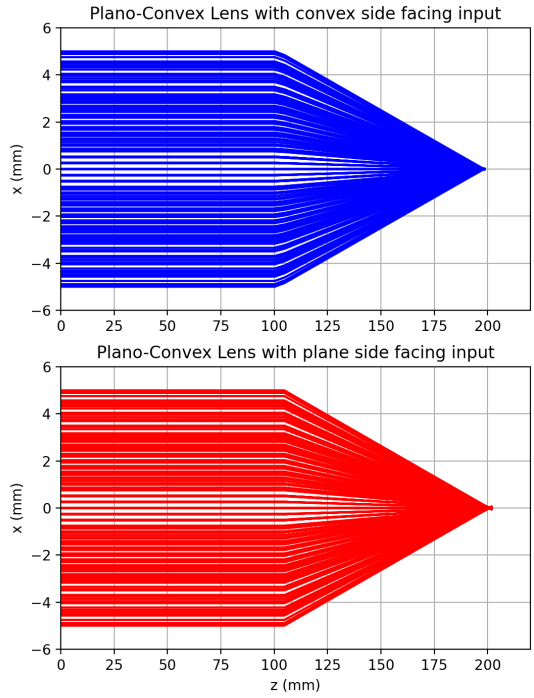

Fig. 5: A plot of a beam of rays shooting at a plano-convex lens in both orientations

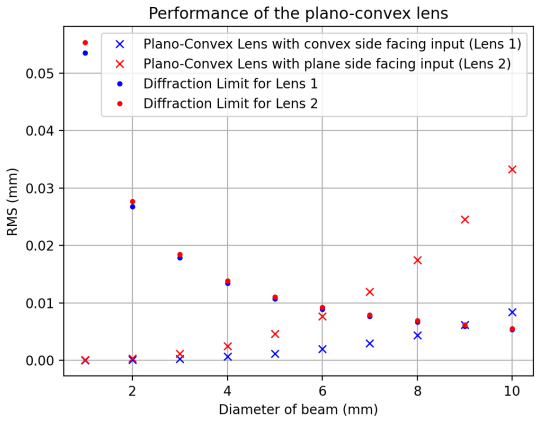

Fig. 6: Performance of the plano-convex lens in both orientation and along with the corresponding diffraction limits for comparison. $\lambda = 558nm$ is used here to calculate the diffraction limits.

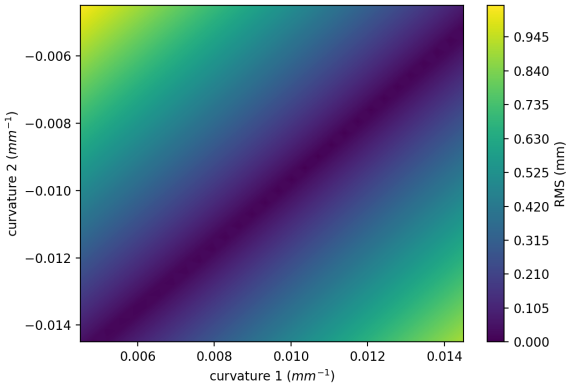

(a) Contour Map (Colour Filled). It shows there is a dark purple region in which different combinations of curvatures gives a small RMS spot radius.

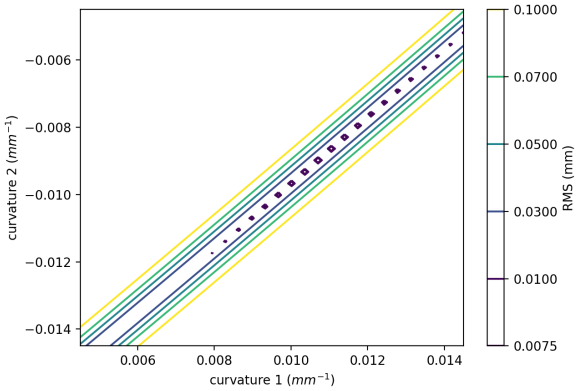

(b) A clearer demonstration of the contours of the contour map in Fig. 7a, which shows that within the valley of low RMS spot radius values there are small minimas in the middle, which could be the better curvature combinations to optimise the lens' performance.

Fig. 7: Contour maps for RMS spot radius against curvatures of the two surfaces, with curvature 1 the curvature for first surface and curvature 2 the curvature for the second surface.